EXPERIMENTAL AND NUMERICAL RESEARCH ON ADSORPTION OF MESUROL SOLUTION IN FIXED-BED CORN SEED TREATMENT

George IPATE[1], Viorel FATU [2], Gheorghe VOICU [3]

In this study, the adsorption of liquid mesurol (with the active substance methiocarb - 1.25 mg/seed, Bayer Cropscience), a repellent insecticide that prevents damage caused by wild animals, birds and insects, is investigated by corn seeds in a fixed bed. To study the adsorption capacity of the seeds on a laboratory scale, they were placed in a 450 ml glass tube with a diameter of 50 mm. An increase in the initial concentration of the solution decreased the adsorption yield, while decreasing the bed length and solution flow rate led to a higher adsorption capacity. The highest seed bed adsorption capacity value of 1.82e-5 mg/g was obtained using a seed bed with a length of 200 mm, and a solution concentration of 48 mg/l at a flow rate of 9 ml/ min. The experimental data obtained by taking samples at an interval of 5 min were tested with the model proposed by Ogata-Banks, which approximates the experimental conditions quite well, even if it also presents some discrepancies. Finally, an adaptive neuro-fuzzy inference system (ANFIS) was used to estimate the adsorption curve, using the data series resulting from the measurements, which indicated a good statistical prediction in terms of relative errors.

Keywords: adsorption, seeds, corn, simulation, neuro-fuzzy.

1. Introduction

Treated seed is defined as that amount of seed to which pesticides are administered to reduce, control or repel disease organisms, insects or other pests that attack the seed [1]. This definition includes the control of pests such as fruit flies (*Oscinella frit*) or birds such as crows (*Corvus corone* or *frugilegus*), pheasants (*Phasianus colchis*), pigeons (*Columba livia f. domestica*) while the seed is in storage and after planting. Corn seeds or grains (barley, oats, rye, wheat and rice), sorghum, millet, soybeans, sugar beets, sunflower, cotton and flax are commonly treated. The seeds of other crops (for example, vegetable seeds) are also covered by

[1] Assoc. Prof., Dept. of Biotechnical Systems, National University of Science and Technology POLITEHNICA Bucharest, Romania, e-mail: george.ipate@upb.ro
[2] PhD Student, Institute of Plant Protection Research and Development, Romania, e-mail: fatu_viorel@yahoo.com
[3] Prof., Dept. of Biotechnical Systems, National University of Science and Technology POLITEHNICA Bucharest, Romania, e-mail: gheorghe.voicu@upb.ro

this plant protection policy. Seed treatment pesticides are applied in either powder, paste or liquid form.

An extremely important food resource and a basic industrial material in the world food economy, corn always occupies an important position. It is also the subject of extensive studies and research regarding the quality of the corn kernels, the yield and the adaptability of the variety. The on-farm seed treatment operation can be broadly defined by formulation, equipment and activity [2]. It generally involves workers operating any on-farm seed treatment equipment, and includes mixing, loading and applying pesticide to untreated seed and any associated tasks such as maintaining treatment equipment and planting treated seed.

In the specialized literature, the transfer of a dissolved substance from a solution to the adsorbent is described by four primary mechanisms [3]. Kinetic analysis and adsorption isotherm of heavy metal ions from aqueous solution using a mixture of corn stalk and tomato waste that were oxidized with nitric acid, performed by Vafakhah et al. (2016) [4], indicated that the kinetic model of the order the second controlled the rate of adsorption. In the study carried out by Ali et all (2022) [5] it was noted that the adsorption mechanism of a dye from an aqueous solution by date seeds is better outlined when the concentration of dissolved substance is low. This is due to the fact that at low initial concentrations, the value of the logarithm of the difference between the equilibrium adsorption capacity and the total one increases exponentially, thus increasing the error function [6, 7].

Today, the two substances applied for decades as a repellent to control bird attacks are no longer used in EU corn cultivation: mesurol with the active ingredient methiocarb (4(methylthio)3,5-xylyl-N-methyl carbamate) and Thiram (tetramethylthiuram sulfide). These substances, according to many studies carried out at international level, show a strong effect of repelling birds without affecting the germination capacity of the seeds [8]. Methiocarb is one of the active substances listed in Regulation (EU) no. 686/2012.

The application of some common methods in the study of complex and non-linear systems in which adsorption processes take place repeatedly encounters certain limitations. To overcome these barriers, the method of analyzing these processes with adaptive neuro-fuzzy inference systems (ANFIS) is very useful in view of the fact that it does not include the physico-chemical phenomena that drive the processes, and as the model is developed, it advances and is well trained, it can estimate extremely easily and quickly the behavior of the system for the subsequent identification of the type of process [9, 10, 11]. In recent studies we find the neuro-fuzzy inference method applied to estimate the adsorption of dichlorophenol on wood-based activated carbon [12], the adsorption of Cu, Cd, and Pb on tropical soils [13] and the biosorption of triglycerides from blood serum [14].

Consequently, this paper aims to study the deposition of methiocarb from the aqueous solution in the mass of corn seeds in an adsorption system with a burst-

type operating regime. The influence of the flow rate, the initial concentration of the solution and the length of the seed bed on the absorption of methiocarb by the adsorbent produced by the seed mass in a fixed bed in a horizontal column at laboratory scale were investigated. In addition, a model based on a neuro-fuzzy inference system was developed to estimate the adsorption of the active substance depending on the parameters of the process.

2. Material and methods

2.1 Adsorbed material

The main data regarding the identity of methiocarb and its physical and chemical properties are presented in Table 1. The dye used in the experiments was a blue ink (ink cyan 644) used in inkjet printing systems and prepared by dissolving water-soluble pigments.

Table 1

Physical and chemical properties of methiocarb

Compound	Melting temperature (^{0}C)	Formula	Chemical Structure	Molecular weight (g/mol)
4-methylthio-3,5-xylyl methylcarbamate	119	$C_{11}H_{15}NO_2S$	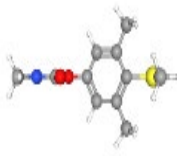	225.31

2.2 The adsorbent material

Maize seeds were used directly for adsorption studies without any chemical treatment. Purchased from the local market in Bucharest, they were randomly selected, dried, cleaned and weighed with a digital scale, after which they were stored for 24 hours at 10°C before being treated with the mesurol solution.

The mass, real density, apparent density (bulk density), porous volume and porosity of the adsorbent were determined by the method proposed in the paper [15]. The actual density ρ_{sem} (kg/m^3) was determined by filling a pycnometer with a well-defined mass of adsorbent mass, m_{sem} and then the pycnometer was adjusted to its volume by adding a well-defined volume of methanol (99% purity) and a been weighed. The calculation of the real density was done using the following relation [16]:

$$\rho = \frac{m_{sem}}{V_{sem}} \quad (1)$$

The bulk density ρ_v (g/cm^3) (bulk density) was determined using a graduated cylinder, which was filled with a certain seed mass (m_{sem}) and then the cylinder was shaken until the seed mass occupied the entire volume of the cylinder. This represents the apparent volume (V_t) of the adsorbent. The bulk density was evaluated using the following relationship [16]:

$$\rho = \frac{m_{sem}}{V_t} \quad (2)$$

The porous volume of the adsorbent is expressed by the porosity Ɛ which was calculated using the results obtained for the real and bulk densities and can be determined by the following relationship [16]:

$$\varepsilon = \frac{\rho_v}{\rho_{sem}} \quad (3)$$

2.3. The experiments on the fixed bed adsorption column

The method of treating seeds in a fixed bed is similar to the practical removal of some constituents from aqueous solutions and presents useful adsorption properties of the adsorbent (seed mass). Fixed-bed adsorption experiments were performed in a laboratory-scale Sohxlet extractor glass column with an inner diameter of 50 mm and a length of 220 mm. The prepared absorbent was introduced into the column with a layer of glass wool at both ends of the bed to ensure good distribution of the liquid solution. It should be noted that the adsorption of methiocarb by glass wool is practically negligible.

A variable amount of methiocarb was mixed with (1 ml) dye (cyan ink 644) and then poured into a glass container (1000 ml) to form an aqueous solution with different concentrations (23, 48, and 86 mg /IT, respectively). All experiments were performed at room temperature (25 °C). The initial adsorbent concentration in the solution was obtained spectrophotometrically at wavelength λ = 450 nm for the mesurol and dye solution.

The treatment solution well homogenized beforehand with a mixer was pumped into the seed bed in the adsorption column in the horizontal direction using a peristaltic pump. The experimental stand is shown in fig. 1(a). The Masterflex L/S digital peristaltic pump includes an Easy-Load II type pump head with 4 rollers, which can dose a volume between 0.28 and 1700 ml/min. It is connected to an LCD graphic screen and an intuitive interface for programming and operating the pump, which allows displaying the dosed volume, cycles and operating time. Four operating modes are available: continuous mode, synchronous dispensing, duplicate dispensing, volume dispensing.

Experiments were performed for different seed bed lengths (100, 150–200 mm), influent methiocarb concentrations (23, 48–86 mg/l) and solution flow rates (6, 9–12 ml/min). The pH of the input solution was adjusted to a value of 5.6, the

optimal value, presented in the study [9]. After the start of the process, the effluent solution sample (which passed the seed bed) was collected at regular time intervals, and then analyzed to obtain the concentration of the active substance by ELISA (Enzyme-Linked Immunosorbent Assay) method in a spectrophotometer SUMAL PE2 (Carl Zeiss) with microplates that allow reading plates with up to 96 wells. In advance, a precise calibration curve was obtained. The samples taken were placed in the spectrophotometer and the precise values of the concentration of the investigated substance were determined according to the absorption of light at the wavelength (λ) of 450 nm fig. 1(b). Finally, the concentration was easily calculated using the calibration curve.

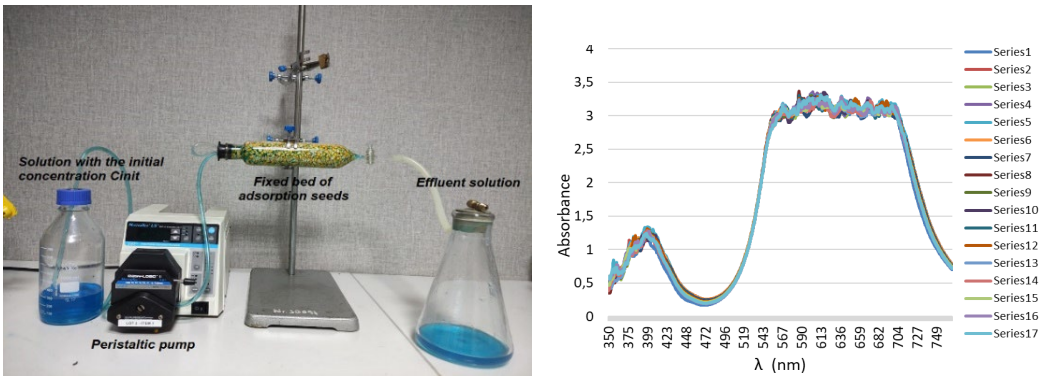

(a) (b)

Fig. 1. The methiocarb adsorption test stand in a fixed bed of seeds (a); spectrophotometric curves for calibration (b)

Aqueous HCl NaOH solutions were used to change the pH of the adsorbate solution. The yield of methiocarb transfer from the solution to the surface of the seeds was calculated as [5,10]:

$$\eta = \frac{C_{init} \times - C_e}{C_{init}} \cdot 100(\%) \quad (4)$$

The adsorption capacity, q_e (mg/g), was estimated with the relation [5,10].

$$q_e = \frac{(C_{init} - C_e) \cdot V}{M} \quad (5)$$

where:

C_{init} and C_e- the initial and equilibrium concentrations (mg/l) of the adsorbate, respectively; V- solution volume (l); M- adsorbent mass (g); q_e- amount adsorbed (mg/g).

The total amount of absorbent retained in the adsorption column can be determined with the relation [5,10]:

$$q_{tot} = \frac{q}{1000} \cdot \int_0^t (C_{init} - C_{fin}) dt \quad (6)$$

where: q - the flow rate of the treatment solution (ml/min).

2.4 Numerical modeling of active solution adsorption

In the field of mechanical engineering, special attention has been paid in recent years to solving the problem of substance dispersion phenomena in the flow through porous media, and the mathematical model of the dynamic behavior of systems has been in the foreground, showing considerable interest.

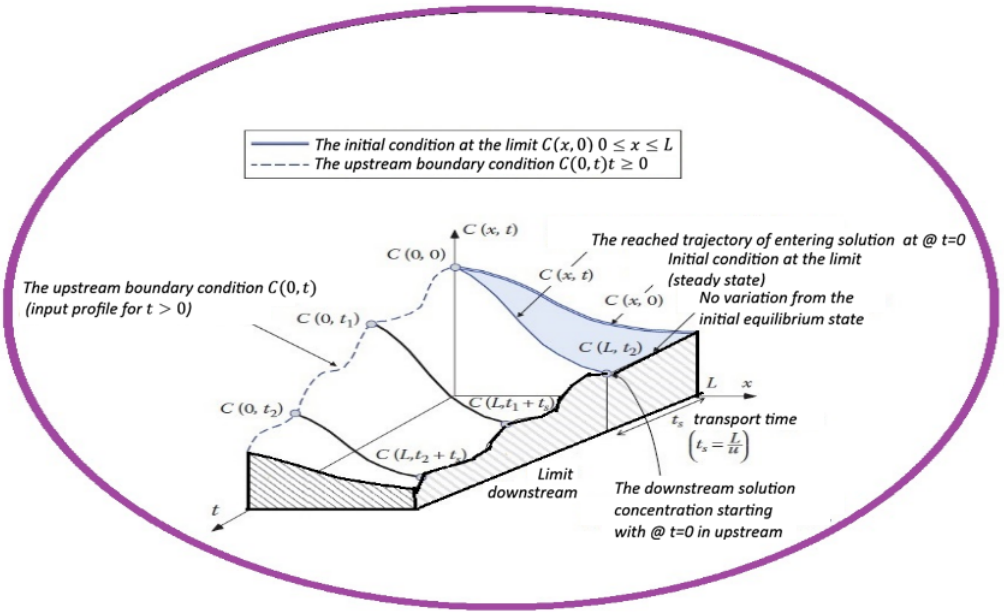

Fig. 2. Modeling the flow process through the adsorption bed and the boundary conditions, [17]

It is assumed that the porous medium is homogeneous and isotropic, that there is mass transfer occurring between the solid and liquid phases, and that also due to microscopic variations in the flow velocity through thin tubes, this can be expressed quantitatively as the product of a coefficient dispersion and concentration gradient. It is also assumed that the flow rate in the porous medium is unidirectional, and the average velocity is constant along the entire length of the flow field (fig.2). The constitutive differential equation is in this case [17]:

$$D \cdot \Delta^2 C = u \cdot \frac{\partial C}{\partial x} + \frac{\partial C}{\partial t} + \frac{\partial F}{\partial t} \tag{7}$$

$$\Delta^2 = \frac{\partial^2}{\partial x^2} + \frac{\partial^2}{\partial y^2} + \frac{\partial^2}{\partial z^2} \tag{8}$$

where: D - dispersion coefficient; C - the concentration of the substance in the solution; u - mean fluid velocity or surface velocity/medium porosity; x - coordinate parallel to the flow. The y, z coordinates are normal to the flow, t is time, and F is the solute concentration in the solid phase. The specific problem considered is that of a semi-infinite medium having a plane source at z=0. Therefore, equation 7 becomes [17]:

$$D \cdot \frac{\partial^2 C}{\partial x^2} - u \cdot \frac{\partial C}{\partial x} = \frac{\partial C}{\partial t} \tag{9}$$

Initially, the saturated fluid of concentration C=0 flows into the medium. At t=0, the plane source concentration changes instantaneously to ($C=C_0$). Thus, the corresponding boundary conditions, shown in fig. 2, are: $C(0,t)=C0$; $t\geq 0$; $C(x,0)=0$; $x\geq 0$; $C(\infty,t)=0$; $t \geq 0$. In this way, the problem then becomes to characterize the concentration of adsorbed substance according to the variables x - space and t - time. To reduce equation 7 to a more familiar form, write [17, 19]:

$$C_{(x,t)} = \Gamma_{(x,t)} \exp\left(u\frac{x}{2D} - u^2\frac{t}{4D}\right) \tag{10}$$

Substituting equation 10 into equation 7 it is obtained:

$$\frac{\partial \Gamma}{\partial t} = D\frac{\partial^2 \Gamma}{\partial x^2} \tag{11}$$

The initial conditions thus transform into:

$$\Gamma_{(0,t)} = C_{init} \cdot exp\left(u^2\frac{t}{4D}\right);\ t\geq 0;\ \Gamma_{(x,0)} = 0; x \geq 0;\ \Gamma_{(\infty,t)} = 0; t \geq 0 \tag{12}$$

For a unidirectional steady flow homogeneous field with constant parameters, the differential mass transport equation (7) for one species has an analytical solution. For the influx of a front with concentration C_{init} ($=C_0$) in a region with concentration C, the extended relationship of the formula proposed in the paper is valid [17,19]:

$$\begin{aligned} c(x,t) = c_0 \exp(-\lambda t)\left(1 - \frac{1}{2}\operatorname{erfc}\left(\frac{Rx-vt}{2\sqrt{DRt}}\right) - \frac{1}{2}\exp\left(\frac{vx}{D}\right)\operatorname{erfc}\left(\frac{Rx+vt}{2\sqrt{DRt}}\right)\right) \\ + \frac{c_{in}}{2}\left(\exp\left(\frac{v-u}{2D}x\right)\operatorname{erfc}\left(\frac{Rx-ut}{2\sqrt{DRt}}\right)\right. \\ \left. + \exp\left(\frac{v+u}{2D}x\right)\operatorname{erfc}\left(\frac{Rx+ut}{2\sqrt{DRt}}\right)\right) \end{aligned} \tag{13}$$

where: $u = (v^2+4\cdot\lambda\cdot R\cdot D)^{0.5}$ - additional parameter depending on the flow type; v – the flow rate of the solution; λ – the adsorbate degradation factor; R – the adsorption retardation factor; erfc– the error function.

Unlike the initial relationship, there are two terms in this case, one that describes the decrease in the initial concentration C_0 ($= C_{init}$) and the second which referred to the change in the input concentration C_{in}. If one of these two concentrations is zero, the relationship becomes simpler because one of the two terms can be omitted. Solving this equation is more convenient when implemented in a dedicated program. To solve the mass transport equation in the porous medium,

the SimTransport simulation program was created - developed by the authors in the GUIDE Toolbox, from the language Matlab, MathWorks - US.

3. Results and discussion

3.1 Characterization of the adsorption material

The results obtained for the determination of 1000 kernels weight, the actual density, bulk density and the porosity of the corn kernels are presented in Table 2. The bulk density of corn kernels determined for a moisture content level with a wet basis of 8.7% was 1245 kg/m^3. The actual density of the seeds was 1450 kg/m^3, only 16.5% higher than the bulk density.

Table 2

Physical properties of maize seeds

Seeds	Moisture content (%, wb)	The real density (kg/m^3)	Bulk density (kg/m^3)	Mass of 1000 grains (g)	Porosity (%)
corn	8.7	1450	1245	250	14.1

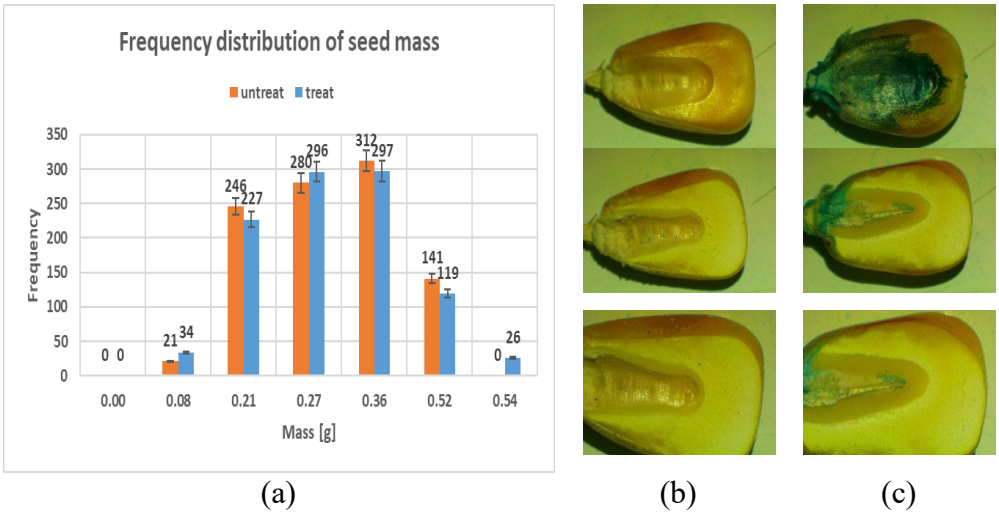

(a) (b) (c)

Fig. 3. Frequency distribution of seed mass before and after treatment with mesurol (a); untreated seeds (b); treated seeds (c)

The porosity of the seed mass was quite high, with a value of 14.1%, estimating that more than 50% of the pore space between the seeds was isolated from the outside, being inaccessible to the treatment solution. The mass of 1000 corn kernels was 250.05 g, with an average of 0.25 g/kernel. The frequency distribution of the seed mass before and after the treatment is presented in fig. 3.

3.2. The influence of the initial concentration of the active substance

The results shows that the solution concentration influences the adsorption process, the percentage decreases from 89.0 % to 77.0 % with an increase in the initial concentration of methiocarb from 23 ppm to 86 ppm, even though the adsorption density increases (fig. 4). In similar experimental conditions for the adsorption of a crystal violet dye on a tamarind seed powder, Patel and Vashi (2010) found in their study [21] that the mass of the given adsorbent can adsorb only a fixed amount of adsorbent. Consequently, the more concentrated the solution, the decrease in the adsorption of methiocarb molecules may be due to the dissolution of the adsorbent species and the change in the pore size, but further evidence is needed on the role played by diffusion between particles in determining the adsorption rate [9, 12, 21].

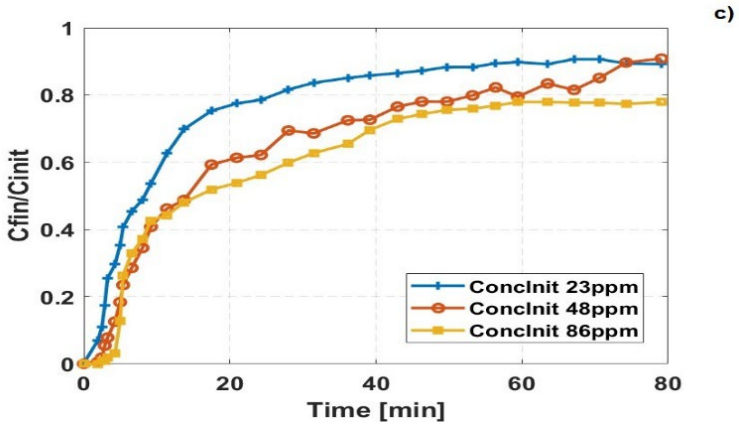

Fig. 4. The influence of treatment solution with different initial concentrations of the active substance at a constant flow rate of 12 ml/ min and a corn kernel bed length in the adsorption column of 200 mm, on the adsorption process

In a way that is somewhat easy to anticipate, the adsorption processes reach the saturation state much faster if the concentration of the solution is higher, mainly due to the fact that for the mass transfer of the methiocarb molecules, a greater driving force is required, generated by the concentration gradient. Thus, the percentage mass transfer yield was dependent on the initial concentration, similar results being obtained by Okoli et al. (2015) and Secar et al. (2004) [22, 23].

3.2. The influence of the flow rate of the solution

The influence of the solution flow rate on the adsorption process was studied under the conditions of a seed bed with a length of 150 mm and an initial concentration of the active substance methiocarb of 48 ppm. Fig. 5 shows the results of the adsorption curves obtained for three different values of the input flow rate of the solution in the adsorption column, namely 6, 9 and 12 mL/min respectively. As can be seen from the data centralizing table (Table 3.), lines 4-6, doubling the

solution flow rate from 6 to 12 mL/min, leads to a rather small decrease in the adsorption yield, from 89.1 % to 84.5%, mainly due to the fact that at higher flow rates the dissolved particles of methiocarb have a much shorter time to diffuse into the free spaces between the seeds or into the pores of the seeds. Simply put, for increased flow rates, the time for the adsorbate in the seed bed to reach the adsorption equilibrium is not long enough, and in this way, methiocarb particles do not have the opportunity to penetrate the pores of the seeds and leave the adsorption column. Similar conclusions can be found in the studies carried out by Nayak and Pal (2009) or Rajeshkannan et all, (2011) [24, 25].

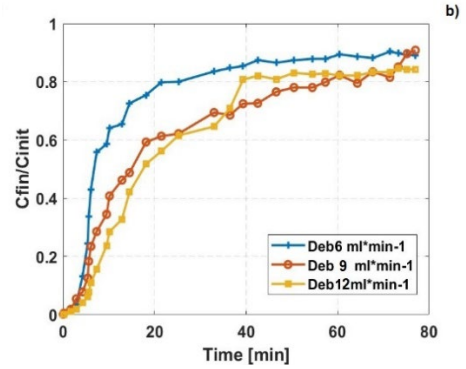

Fig. 5. The influence of the solution flow on the adsorption process

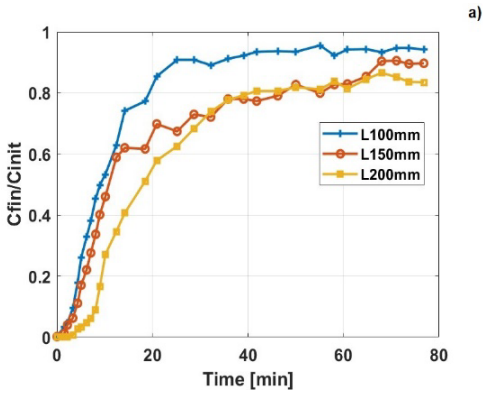

Fig. 6. The influence of the adsorption bed length on the adsorption process

Another argument, presented by Santhy and Selvapathy (2006) in their work [26], is that some of the molecules adsorbed on the surface of the adsorbent can be desorbed due to the increased flow speed of the solution through the column. However, there are several works in the literature on the continuous adsorption of particles in a fixed bed of seeds, among which we mention only the one by Sananmuanga and Cha-un [27], which demonstrate that in addition to the flow rate, a significant influence on the adsorption capacity of the seeds also has the optimal temperature of the solution. The specific S-shapes of the adsorption curves also called penetration curves of dissolved particles in the pore space of the absorbent layer can be observed in fig. 5.

3.3. The influence of the length of the seed bed

Adsorption bed length means the distance an adsorbent material covers in an adsorption process. This length can significantly influence the efficiency and performance of an adsorption system and can vary depending on several factors.

Figure 6 shows a graph of the variation of the ratio between the adsorbate concentration and the initial concentration of the Cfin/Cinit solution, obtained for the adsorption of methiocarb on corn seeds for different lengths of the fixed bed of

100, 150 and 200 mm (corresponding to masses of 245, 367 and 500 g of adsorbent), at a constant flow rate of 6 mL/min and an inlet concentration of 23 mg/L.

If the adsorption bed is too short, it may not provide enough time for the substances to be adsorbed on the adsorbent surface in significant quantities. This can lead to a reduced efficiency of the adsorption process. On the other hand, too long an adsorption bed can lead to an unnecessary waste of time and energy. It is interesting and easy to see both from fig. 6 as well as table 3 that the methiocarb adsorption efficiency decreased with the increase in the length of the seed bed, from a value of 94.32% for the bed length of 100 mm, to a value of 89% for the bed length of 150 mm, and respectively, at the value of 83.4% for the adsorbent bed with a length of 200 mm. Consequently, a lower length of the seedbed was favorable to the adsorption capacity of methiocarb, in accordance with those mentioned by other authors [5, 9, 22, 24-27].

The length of the adsorption bed determines the contact time between the gas or liquid to be adsorbed and the adsorbent. The longer the adsorption bed, the longer the contact time, which can increase the chances of the adsorbent capturing the desired substance. However, this can be a double-edged sword, as it can also increase the risk of unwanted adsorption.

The uniform distribution of the adsorbent along the entire length of the adsorption bed allows an efficient distribution of the adsorbent. If there are areas of different adsorbent density in the adsorption bed, this can lead to significant variations in process efficiency, causing a channeling effect, the solution usually finds a flow path past the column wall where there are more voids, even if in an attempt to distribute the liquid solution as constantly as possible in time and space, a layer of cotton wool was used at the entrance to the glass column.

Table 3

The experimental results obtained in the process conditions (T = 25 °C și pH = 5.7)

No	L (mm)	Q (mL min^{-1})	C_{init} (mg /L)	time (min)	q_{total} (mg)	q_{eq} (mg/g)	η_e (%)	η_{sn} (%)	Ɛ (%)
1	100	6	23	80	1.73E-03	7.08E-06	94.32	97.6	3.48
2	150	6	23	80	1.44E-03	5.87E-06	89	92.3	3.71
3	200	6	23	80	1.69E-03	6.91E-06	83.4	88.5	6.12
4	150	6	48	80	4.30E-03	1.76E-05	89.1	91.6	2.81
5	150	9	48	80	6.20E-03	1.69E-05	85.8	88.7	3.38
6	150	12	48	80	7.25E-03	1.48E-05	84.26	87.5	3.85
7	200	12	23	80	4.04E-03	8.27E-06	89.1	92.4	3.70
8	200	12	48	80	8.89E-03	1.82E-05	80.7	83.6	3.59
9	200	12	86	80	1.899e-6	3.84E-05	77	80.5	4.55

Another possible explanation found in the literature regarding fixed bed adsorption processes is that since there are no changes in the temperature of the solution, the value of the adsorption energy is below the value of 8kJ/mol, and the adsorption process takes place only physically; for values between 8 and 16kJ/mol

of the free energy, encountered in cases where the temperature of the solution is increased, then a chemical adsorption also takes place [25].

3.4. Numerical modeling

The graphical user interface of the simulation program made in the Matlab programming environment consists of various components such as windows, buttons, text boxes, drop-down lists, panels, menu bars and many others used to display information and to allows users to interact quickly and efficiently with the application. Launching the application is done by pressing the "Run" button.

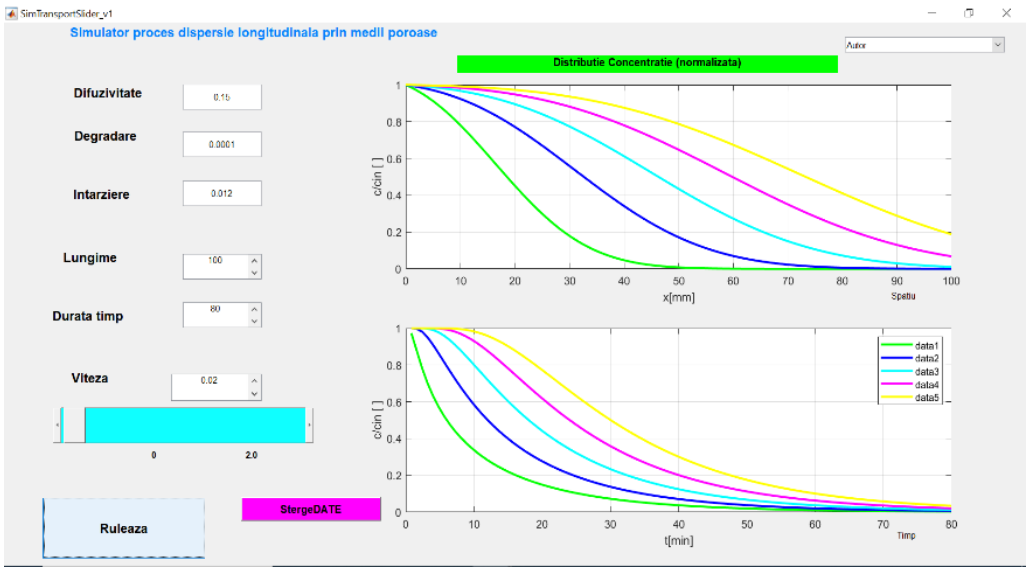

Fig. 7. Interactive graphical user interface (GUI) of the simulation program created for fixed bed adsorption - graphical results

In the graph at the top of the graphical interface of the application presented in fig.7, in the first coordinate system, the ratio of concentration values is calculated for each of the 5 equidistant locations chosen along the model axis, i.e. along the length of the seed bed. After making the calculations, the corresponding curve is drawn. The graphs presented in the second coordinate system (bottom of the interface) represent the calculations performed for the ratio of the concentration values at each of the 5 equidistant time intervals chosen.

Following the numerical simulation, the absorption yields were obtained for the process in a fixed bed of seeds depending on the different experimental conditions. The results obtained by numerical simulation were compared with the values determined experimentally (table 3, column 8), calculating the percentage deviation (error) with the relation [28]:

$$\varepsilon = \frac{\eta_{e-\eta_{sn}}}{\eta_{sn}} \cdot 100(\%) \qquad (14)$$

where: Ɛ - the percentage error or deviation; η_e - the value of the adsorption efficiency determined experimentally; η_{sn} - the value of the adsorption yield determined by numerical simulation.

The percentage deviation values are presented in table 3, column 10. From the results presented in figure 8 and table 3, it can be seen that the maximum error was 6.12% for experiment 3, in which the length of the seed bed had the highest value, and the concentration of the active substance was the highest. It is also noted that larger deviations appear in experiments 9 and 6. A possible source of the error between the experimental and calculated values is that the simulations are based on a mathematical model that contains assumptions and approximations which, if they are not sufficiently precise or do not accurately reflect the real situation, may lead to the appearance of these errors.

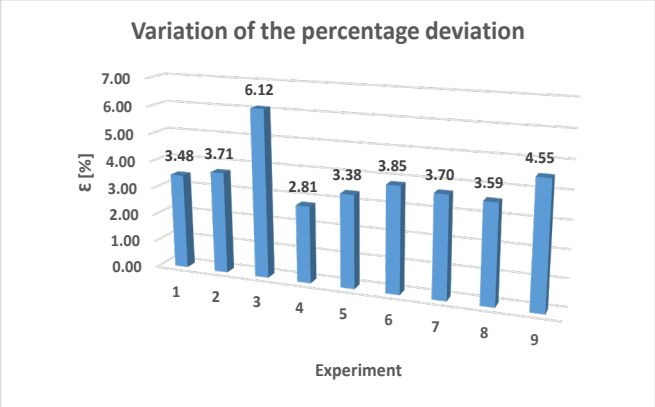

Fig. 8. The percentage deviation of the fixed bed adsorption yield

Another particularly important reason why errors can appear in numerical simulations is the quality of the input data used in the simulation is essential. If the data used to initialize the simulation is inaccurate or incomplete, this can lead to errors in the simulated results.

3.5. The neuro-fuzzy adaptive inference system

ANFIS (Adaptive Neuro-Fuzzy Inference System) neuro-fuzzy model is an artificial intelligence technology that combines elements of artificial neural networks (ANN) and fuzzy systems to build an inference system capable of modeling and understanding complex relationships between variables of input and output of a system [29, 30].

An important feature of an ANFIS model is that it uses concepts from fuzzy systems theory to represent human knowledge and to translate this knowledge into a mathematical model. Fuzzy systems allow the expression of ambiguity and uncertainty in the decision-making process. They use fuzzy sets, membership

functions and fuzzy rules to define inference rules [31, 32]. Artificial Neural Networks (ANN) are components used by the inference system to optimize and adjust model parameters based on training data. In particular, ANFIS uses a feedforward neural network structure to perform adaptive fuzzy inference. It involves neuron-like nodes that perform the calculations and feed the signals forward.

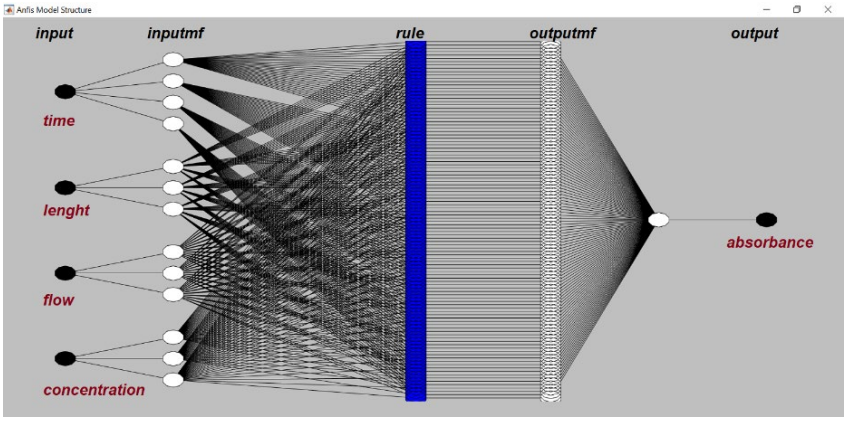

Fig. 9. Structure of the ANFIS model, a 6-layer neuro-fuzzy network without reverse connections

In the present study, we used one of the most well-known models in this field proposed in the paper [29]. Figure 9 shows a typical ANFIS structure that consists of six distinct layers. The Sugeno first-order fuzzy model considered four inputs (time, bed length, flow and initial solution concentration) and an output "absorbent" of the effluent sample. The output layer combines the fuzzy outputs of the rules according to specific weights to produce final results. The proposed model uses adaptive learning techniques to adjust the weights and membership functions of the fuzzy rules to best match the training data. This adaptive learning is based on the hybrid optimization algorithm or Levenberg-Marquardt method.

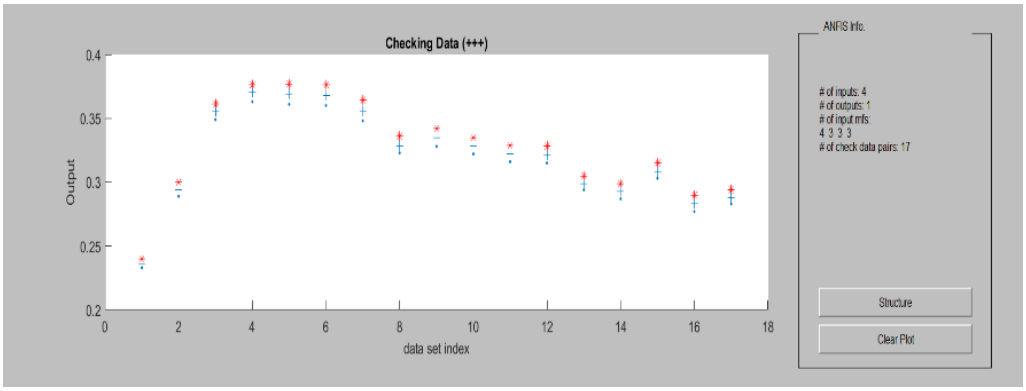

Fig. 10. Training, validation and verification of the ANFIS model

The ANFIS method requires training data to adjust the model parameters. This data consists of pairs of known inputs and outputs to guide learning and adaptation. The average values of the experimental data obtained by measuring the absorbance of the solution at the exit from the adsorption column were divided into three groups, each with 5 sets of data, composed of 17 pairs [29]; the first group with is used for training/training, the second, for model validation, and the third group, is used for ANFIS model verification. The comparison of the output data from the inference model with the data from the 3 groups is presented in fig.10. In this figure, the points marked with red stars represent the output data from the neuro-fuzzy model, the points marked with a blue cross represent the data from the verification group, and the blue points are the data from the validation group.

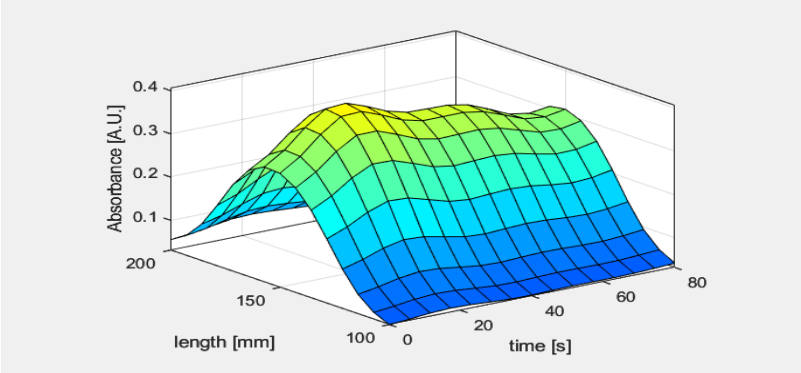

Fig. 11. Graphic representation of the output data from the ANFIS model

The graphic representation of the output data from the model, in the form of the surface shown in fig. 11, is non-linear and monotonic and illustrates that the two sets of data, the length of the adsorption bed and the time, form the optimal combination of two input variables. An absorbance peak of 0.35 [a.u.] can be observed after about 20 minutes from the start of the process for a seed bed with a length of 150 mm.

4. Conclusions

In this work, the adsorption capacity of the methiocarb substance by the corn seeds was investigated, in order to obtain an alternative treatment with low cost and effective in a burst type of operation. Since a portion of the pore spaces between the seeds is inaccessible to the treatment solution, it is possible that the adsorption of the active substance will be very reduced, and in this way, the seeds will have a lower level of protection against pests. It can also be observed that the porosity, real and bulk density of the seeds represent important physical factors that influence their resistance to the development of microorganisms or fungi.

Another parameter, which together with the other thermodynamic parameters will be the object of future research, is the mean free energy, which can reveal the nature of the adsorption mechanisms.

An adaptive interference model is a solid approach to solving problems involving uncertainty and complexity, being able to integrate human knowledge (in the form of fuzzy rules) with the machine learning capabilities of artificial neural networks to create accurate and adaptive models.

Finally, simulation errors may be unavoidable to some extent, but efforts to minimize and understand them are essential to make simulations more useful and relevant in their specific context.

REFERENCES

[1]. *A. Lentola, C. Giorio, S. Bogialli, et al.* Methiocarb metabolites are systemically distributed throughout corn plants grown from coated seeds. Environ Chem Lett, **vol .19**, 2021, pp. 1887–1892. https://doi.org/10.1007/s10311-020-01098-3

[2]. *M. Crowley, J. Dawson, K. Lowe, B. VanDeusen,* Standard Operating Procedures (SOPs) for Seed Treatment, United States Environmental Protection Agency, January, 2022. https://www.epa.gov/system/files/documents/2022-01/exposac-policy-14_seed-treatment-exposure-data.pdf

[3]. *S.K. Lagergren*, About the theory of so-called adsorption of soluble substances, Sven. Vetenskapsakad. Handingarl, **vol. 24**, 1898, pp. 1–39.

[4]. *S. Vafakhah, M. E. Bahrololoom, M. Saeedikhani*, Adsorption Kinetics of Cupric Ions on Mixture of Modified Corn Stalk and Modified Tomato Waste, Journal of Water Resource and Protection, **vol. 8,** No.13, November 28, 2016

[5]. N.*S. Ali, N.M. Jabbarb, S.M. Alardhic, H.Sh. Majdid, T.M. Albayati*, Adsorption of methyl violet dye on to a prepared bio-adsorbent from date seeds: isotherm, kinetics, and thermodynamic studies, Heliyon, **vol. 8**, e10276, 2022.

[6]. *S. Azizian*, Kinetic models of sorption: a theoretical analysis, J. Colloid Interface Sci., **vol. 276**, (1), 2004, pp. 47–52.

[7] *A.T. Khadim, T.M. Albayati, M. Noori, C. Saady*, Desulfurization of actual diesel fuel onto modified mesoporous material Co/MCM-41, Environ. Nanotechnol. Monit. Manag., **vol. 17**, 100635, 2022.

[8]. *M. Arena, D. Auteri, S. Barmaz et all*., Peer review of the pesticide risk assessment of the active substance methiocarb, EFSA Journal, **vol. 16**, No.10, 2018, 5429.

[9]. *M.H. Marzbali, M. Esmaieli*, Fixed bed adsorption of tetracycline on a mesoporous activated carbon:Experimental study and neuro-fuzzy modeling, Journal of Applied Research and Technology, **vol. 15**, 2017, pp. 454–463.

[10]. *M. Ghaedi, R. Hosaininia, A.M. Ghaedi, A. Vafaei, F. Taghizadeh*, Adaptive neuro-fuzzy inference system model for adsorption of 1,3,4-thiadiazole-2,5-dithiol onto gold nanoparticales-activated carbon, Spectrochimica Acta, Part A: Molecular and Biomolecular Spectroscopy, **vol. 131**, 15, October, 2014, pp. 606-614.

[11]. *K. Aghajani, H.A. Tayebi*, Spectrochimica Acta, Part A: Molecular and Biomolecular Spectroscopy, Vol. 171, 15, January, 2017, pp. 439-448.

[12]. *A. Alver, E. Baştürk, Ş. Tulun, I. Şimşek*, Adaptive neuro-fuzzy inference system modeling of 2,4-dichlorophenol adsorption on wood-based activated carbon, Environmental Progress & Sustainable Energy, **vol. 39**, 5, 2020. https://doi.org/10.1002/ep.13413
[13]. *B. K. Agbaogun, B. I. Olu-Owolabi, H. Buddenbaum, K. Fischer*, Adaptive neuro-fuzzy inference system (ANFIS) and multiple linear regression (MLR) modelling of Cu, Cd, and Pb adsorption onto tropical soils, Environ Sci Pollut Res 30, 31085–31101 (2023). https://doi.org/10.1007/s11356-022-24296-8
[14]. *E. Salehi, S. Tahmasbi, V. Tahmasbi, M. Rahimi*, Application of the Adaptive Neuro-Fuzzy Inference System (ANFIS) and Sobol Approaches for Modeling and Sensitivity Analysis of the Biosorption of Triglyceride from the Blood Serum, Iranian Journal of Chemical Engineering, **vol. 19**, 1, 51-65, 2022. https://doi.org/10.22034/ijche.2022.343384.1437
[15]. *C.S. Chung*, Measuring density and porosity of grain kernels using a gas pycnometer, Cereal Chem., **vol. 65**, 1, pp. 13-15, 1987.
[16]. *B. Hayoun, M. Bourouina, M. Pazos, M.A. Sanromán, S. Bourouina-Bacha*, Equilibrium Study, Modeling and Optimization of Model Drug Adsorption Process by Sunflower Seed Shells. Appl. Sci. **vol. 10**, 2020, pp. 3271. https://doi.org/10.3390/app10093271
[17]. *E. Holzbecher*, Environmental Modeling using MATLAB - sec. edition, Springer Berlin, 2013
[18]. *W. Kinzelbach*, Numerische Methoden zur Modellierung des Transports von Schadstoffen im Grundwasser, Oldenbourg, Munchen, 1987.
[19]. *A. Ogata, R.B. Banks*, A Solution of the Differential Equation of Longitudinal Dispersion in Porous Media, US Geological Survey, Professional Paper No. 411-A, 1961.
[20]. *G. Ipate, D.N. Ipate*, Modelarea si Simularea Factorilor de Mediu (Modeling and Simulation of Environmental Factors), ISBN 978-973-0-37182-6, Bucuresti, 2022.
[21]. *H. Patel, R.T. Vashi*, Adsorption of crystal violet dye onto Tamarind seed powder, E-Journal of Chemistry, **vol. 7,** 3, 2010, pp. 975-984.
[22]. *C.A. Okoli, O.D. Onukwuli, C.F.Okey-Onyesolu, C.C. Okoye*, Adsorptive removal of dyes from synthetic wastewater using activated carbon from tamarind seed, European Scientific Journal, June, **vol.11**, 18, ISSN: 1857 – 7881 (Print) e - ISSN 1857- 7431, 2015.
[23]. *M. Sekar, V. Sakthi, S. Rengaraj*, Kinetics and Equilibrium Adsorption Study of Lead (II) Onto Activated Carbon Prepared from Coconut Shell, Journal of Colloid and Interface Science, **vol. 279,** 2, 2004, pp. 307-313.
[24]. *A. K. Nayak, A. Pal*, Rapid and high-performance adsorptive removal of hazardous acridine orange from aqueous environment using Abelmoschus esculentus seed powder: Single- and multi-parameter optimization studies, Journal of Environmental Management, **vol. 217**, 1 July, 2018, pp. 573-591.
[25]. *R. Rajeshkannan, M. Rajasimman, N. Rajamohan*, Decolourization of malachite green using tamarind seed: optimization, isotherm and kinetic studies, Chemical Industry & Chemical Engineering Quarterly, **vol. 17**, 1, 2011, pp. 67−79.
[26]. *K. Santhy, P. Selvapathy,* Removal of reactive dyes from wastewater by adsorption on coir pith activated carbon, Bioresource Technology, **vol. 97**, 2006, pp. 1329-1336.
[27]. *R. Sananmuanga, N. Cha-un*, Physical Characteristics and Adsorption Properties for Reactive Dyes of Char and Activated Carbon Prepared from Mangosteen Peel and Tamarind Seed, Naresuan University Journal, **vol. 15,** 1, 2007, pp. 9-16.
[28]. *C. Haţiegan*, Identificarea defectelor în plăci elastice subţiri prin analiză modală, Teza de doctorat, (Identification of defects in thin elastic plates by means of modal analysis, PhD Thesis), Universitatea „Eftimie Murgu" din Reşiţa, Reşiţa, 2013.
[29]. *G. Ipate, C. Ciobanu, P. Tudor, I. Gageanu, D. Cujbescu, Manaila, F.*, Adaptive neuro-fuzzy model for the control system of the clinker grinding process in ball mills in cement factories, INMATEH - Agricultural Engineering, **vol. 68**, 3, 2022, pp. 579–588.

[30]. *N. Constantin*, Rețele neuro-fuzzy cu auto-organizare pentru sisteme de reglare adaptivă (Self-organizing neuro-fuzzy networks for adaptive control systems), Revista Română de Informatică şi Automatică, **vol. 13**, 4, 2003, pp. 48-55.
[31]. *V. Cărbune*, Adaptive hardware architectures for neuro-fuzzy systems with self-organization, Ph.D. thesis, Universitatea Tehnica a Moldovei, Chisinau, 2020.
[32]. *** https://uk.mathworks.com/help/fuzzy/dsigmf.html..